J Comput Neurosci (2011) 31:285–304
DOI 10.1007/s10827-010-0308-6

Leader neurons in leaky integrate and fire neural network simulations

Cyrille Zbinden

Received: 16 April 2010 / Revised: 14 December 2010 / Accepted: 16 December 2010 / Published online: 14 January 2011

Abstract In this paper, we highlight the topological properties of leader neurons whose existence is an experimental fact. Several experimental studies show the existence of leader neurons in population bursts of activity in 2D living neural networks (Eytan and Marom, J Neurosci 26(33):8465–8476, 2006; Eckmann et al., New J Phys 10(015011), 2008). A leader neuron is defined as a neuron which fires at the beginning of a burst (respectively network spike) more often than we expect by chance considering its mean firing rate. This means that leader neurons have some burst triggering power beyond a chance-level statistical effect. In this study, we characterize these leader neuron properties. This naturally leads us to simulate neural 2D networks. To build our simulations, we choose the leaky integrate and fire (lIF) neuron model (Gerstner and Kistler 2002; Cessac, J Math Biol 56(3):311–345, 2008), which allows fast simulations (Izhikevich, IEEE Trans Neural Netw 15(5):1063–1070, 2004; Gerstner and Naud, Science 326:379–380, 2009). The dynamics of our lIF model has got stable leader neurons in the burst population that we simulate. These leader neurons are excitatory neurons and have a low membrane potential firing threshold. Except for these two first properties, the conditions required for a neuron to be a leader neuron are difficult to identify and seem to depend on several parameters involved in the simulations themselves. However, a detailed linear analysis shows a trend of the properties required for a neuron to be a leader neuron. Our main finding is: A leader neuron sends signals to many excitatory neurons as well as to few inhibitory neurons and a leader neuron receives only signals from few other excitatory neurons. Our linear analysis exhibits five essential properties of leader neurons each with different relative importance. This means that considering a given neural network with a fixed mean number of connections per neuron, our analysis gives us a way of predicting which neuron is a good leader neuron and which is not. Our prediction formula correctly assesses leadership for at least ninety percent of neurons.

Keywords Simulation · Model · Neuron · Burst · Leader · Integrate and fire

Action Editor: Wulfram Gerstner

C. Zbinden (✉)
Département de Physique Théorique, Université de Genève, 1211, Genève 4, Switzerland
e-mail: cyrille.zbinden@unige.ch

1 Introduction

Disassociated *in vitro* rat brain neuron cultures show, under a variety of experimental contexts, a spontaneous electrical activity. This activity manifests itself by a rapid succession of ignitions of a large fraction of neurons named collective bursts (or network spikes) (Tscherter et al. 2001; Maeda et al. 1995; Droge et al. 1986; Wagenaar et al. 2006a). This bursting activity can be measured, for example, by multi-electrode array methods (Eytan and Marom 2006; Eckmann et al. 2008; Wagenaar et al. 2006b) or by fluorescence (Soriano et al. 2008). The study of the initiators of these bursts is one of the conceptual problems underlying the spontaneous electrical activity. As Eytan and

Marom (2006) said, "cognitive processes depend on the synchronization of the electrical activity within and between neuronal assemblies. *In vivo* measurements show that the size of individual assemblies depends on their function and varies considerably, but the timescale of the assembly activation is in the range of 0.1–0.2 s and is primarily independent of the assembly size." In this paper, the *in vitro* experiments we model permit us to characterize the process underlying the timescale of synchronization. Precisely, we focus on the initiators of bursts by regarding their topology of connectivity.

Regarding the initiators of bursts, the Eytan and Marom study (Eytan and Marom 2006) showed that some "first to fire" cells exist. Later (Eckmann et al. 2008), through a detailed analysis of data obtained by the multi-electrode array methods, established that some cells are triggering bursts beyond a simple statistical effect of being the first. These particular cells are called *leaders*. The analysis (Eckmann et al. 2008) indicates that the long term dynamics of the leaders is relatively robust, evolving with a half-life of about one day. Eckmann et al. (2008) also shows that these leaders are not only the main initiators of bursts, but, the burst itself carries traces (or hints) indicating which of the leaders has initiated the burst. In this respect, one can view the culture as an amplifier of the signal emitted by the leaders.

It is clear that the scenario described above calls for a theoretical explanation. One of the ways pursued is the one of (bootstrap) percolation in random networks (Eckmann and Tlusty 2009) which gives insights into the spread of the initial ignition and distinguishes between localized and de-localized spreading. In this picture, the burst itself is viewed as the "giant component" of the percolation process, and this picture is verified from many different angles (Soriano et al. 2008).

In this paper, we address the delicate question of what makes a neuron a leader. Is it stimulation? Activity threshold? Special connectivity properties of the network? The natural way of reaching this aim theoretically is to simulate a random neural network. Our results show that leadership results from of a combination of several natural parameters of the neuron which can be quantified by a simple relation. We obtain these results by a simple model of a randomly connected network with the usual leaky integrate and fire (Gerstner and Kistler 2002) mechanism for ignition of neurons. This well known model (Cessac 2008) is tested in numerical event-based simulations that provide, in principle, unbiased simulations (Cessac et al. 2008). This model only takes into account simple properties of neurons (integrate and fire) (Izhikevich 2004; Gerstner and Naud 2009) but it suffices to reproduce basically all the findings of Eckmann et al. (2008). Thus we trade realism for conceptual simplicity, but in this kind of investigations the complexity comes from the neural network as a whole and not from the neuron model.

The results of our simulations can be presented as follows: to each neuron one can assign a leadership score and neurons with the highest scores are leaders. It turns out that leaders can be characterized as being excitatory neurons and having a low membrane potential firing threshold. Apart from these two first properties, the conditions required for a neuron to be a leader are difficult to identify and depend on several parameters involved in the simulations themselves. The main finding of this paper is a formula for the leadership score that exhibits five essential properties for leaders with relative importance. This formula gives a very good statistical prediction. Therefore, we can conclude that leadership is a random effect, and that leaders are formed naturally from a balanced combination of inputs, outputs, their local neighborhood and their own properties. Basically a leader sends a signal to a lot of excitatory neurons as well as to a few inhibitory neurons and a leader receives only a few signals from other excitatory neurons.

2 The simulations

In this section we explain how we construct our leaky integrate and fire simulations and which parameters we use.

2.1 Building the simulations

A single neuron is already a complex biological object. But, basically, neurons are electrically excitable cells that are composed of a soma (cell body), a dendritic tree and an axon. Dendrites and axons connect to each other (through synapses) to create a neural network. While the 2D topology of the *in vitro* dissociated cultures (Eckmann et al. 2008) is not known, we can still construct models with parameters taken from the many experimentally known properties of neuronal cultures (Eckmann et al. 2007). In this paper, we choose a geometry and some rules that produce the rule of connections between neurons (Zbinden 2010) or construct a random neural network with a fixed mean number of connections per neuron.

Our simulations are built as follows. First we construct a matrix of synaptic weights W that represents a random neural network of $N \in \mathbb{N}$ neurons where N is a parameter and $\sqrt{N} \in \mathbb{N}$ as so we can consider that the neurons are placed on a grid $\{(x, y) \in \mathbb{N}^2 |$

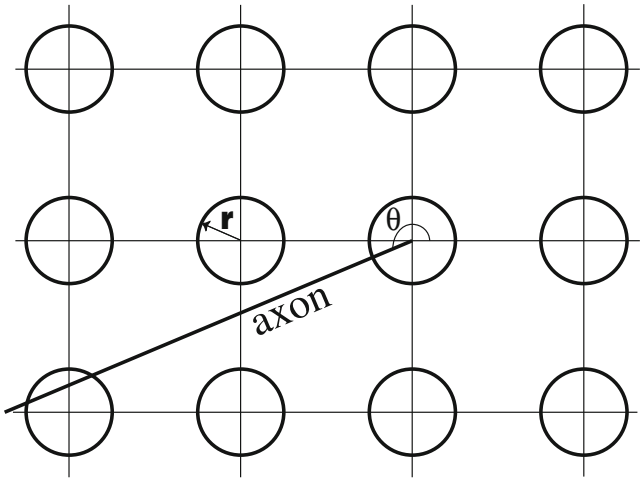

Fig. 1 A 3×4 neurons rectangle. Each neuron is a circle with a radius $\mathsf{r} \in \mathbb{R}_+$ (dendrites), in this figure $\mathsf{r} < 1$. The axon of one of the neurons is drawn. We see that this neuron is connected to the neuron on the left of the bottom row. Note that the axon direction is given by $\theta \in [0,\ 2\pi)$. Note also that if $\mathsf{r} \geq 1$, unlike in this figure, then we automatically have nearest neighbor connections

$x, y \leq \sqrt{N}\} \subset \mathbb{R}^2$ with periodic boundary conditions. In the Euclidean geometry of $\mathbb{R}^2$, we consider that every neuron n $(n = 1, 2, \ldots, N)$ is a circle of radius $\mathsf{r} \in \mathbb{R}_+$ (equivalent to the spatial extension of the dendrites). Each axon has a length $\ell \in \mathbb{R}_+$, approximately Gaussian distributed (with probability density function close[1] to $f(\ell,\ L) = \frac{1}{\lambda\sqrt{2\pi}} e^{-\frac{(\ell - L)^2}{2\lambda^2}}$ where $L \in \mathbb{R}_+$ is the mean axon length and $\lambda = \frac{1}{3}\min(L - 1, \frac{2}{3}\sqrt{N} - L)$ is the standard deviation (and $1 < L < \frac{2}{3}\sqrt{N}$)). In our simulations, the neuron spatial parameters are the dendrite size r and the mean axon length L. To every axon, we also associate a direction (respectively an angle) $\theta \in [0,\ 2\pi)$ uniformly distributed (with probability density function $g(\theta) = \frac{1}{2\pi}$). Figure 1 illustrates the network geometry.

To construct the matrix $W \in \mathrm{M}_N(\mathbb{R})$, we proceed as follows: If the axon (with finite length ℓ, without width and angle θ (respectively direction)) of the neuron m $(m = 1, \ldots, N)$ intersects the circle (dendrites) of the neuron $n \neq m$ $(n = 1, \ldots, N)$ then the connection exists (i.e., $W_{nm} \neq 0$), otherwise $W_{nm} = 0$. The biological knowledge tells us that the connections between neurons is oriented (electrical impulses move from axons to dendrites). Thus we have a non-symmetric matrix of synaptic weights W representing the neural network.

A fix parameter $\mathsf{w} \in \mathbb{R}_+$ named the synaptic weight is the value we give to W_{nm} when the connection exists (i.e., $W_{nm} \neq 0$). Note that, in reality, some neurons are inhibitors. For these, we use a negative synaptic weight $-\mathsf{w} \in \mathbb{R}_-$. In our simulations the proportion $r \in [0,\ 1]$ of inhibitory neurons is also a parameter.

To simplify the terminology, if $W_{nm} \neq 0$, we will say that the neuron n is the son of the neuron m and the neuron m is the father of the neuron n. One given neuron can have more than one father and more than one son. Of course, a given neuron can be both, father and son of another neuron.

Roughly, the matrix of synaptic weights represent a random network even if this particular network is not a network in which the probability of connections between all pairs of neurons is equal.[2] Here since the considered experiments (Eytan and Marom 2006; Eckmann et al. 2008) are 2D one, we propose a 2D geometry to construct neural networks. Precisely, in the experiments, the network is built from dissociated neurons, then the connectivity is determined by a spatial search process during the network growth, which is for all practical purposes a random network. This is the basic reason for the network geometry that we propose. Clearly, once more is known about the experimental topology, differences between the model we propose and the experiments could appear.

In general, the word "random graph" is reserved for certain classes of graphs, with a probability measure on them. For example, the class $G_{N,p}$ describes the set of graphs with N nodes and each possible link chosen to exist with probability p. The class of graphs chosen in this paper is a random graph, but the measure is not a standard one. The measure is actually described by the process by which the graph is built and has got several random components. First, the nodes (respectively the neurons) have properties (like the membrane potential firing threshold; see below) which are chosen randomly with a certain distribution. Second, the axons are random in two ways: their direction, and their length. On the other hand, the length is chosen from experimentally known data and finally the number of connections is modeled after the work (Eckmann et al. 2007), as we explain below.

Once the matrix of synaptic weights is constructed we assign two real values to each neuron n: V_n^* the membrane potential firing threshold and $V_n(t)$ the membrane potential which depends on the time $t \in \mathbb{R}_+$.

[1] Negative axon lengths are not allowed and we impose a maximum length of $\frac{2}{3}\sqrt{N}$ for each axon. With this last condition, no axon can cover all the network in any direction. The rationale for this choice is that, in the experiments (Eckmann et al. 2008), probably no axon covers all the test tube in any given direction.

[2] Random network in which the probability of connections between all pairs of neurons is equal are also studied in this paper. Table 3 shows also results concerning this particular kind of random networks.

Without loss of generality, we can consider that the membrane potential[3] fluctuates roughly between 0 and $\langle V^* \rangle = 1$ (where $\langle V^* \rangle$ is the mean of all the neuron membrane potential firing thresholds). The time evolution of the membrane potential $V_n(t)$ is computed using the leaky integrate and fire (Gerstner and Kistler 2002) neuron model.

The dynamics is the following, every neuron n (respectively every membrane potential $V_n(t)$) which integrates the electrical signal it receives from the other neurons is able to fire (when $V_n(t) > V_n^*$) and then sends a signal to the other neurons. Just after firing the membrane potential is reset to 0. The membrane potential also decreases with a leaky time τ (loss of memory).

More precisely, the membrane potential evolution equation of the neuron n is the evolution equation of a leaky integrate and fire neuron model (Gerstner and Kistler 2002)

$$V_n(t+dt) = \underbrace{V_n(t)e^{-\frac{dt}{\tau}}}_{\text{Loss of memory}} \underbrace{(1-\chi_n[V_n(t)])}_{\text{Reset after firing}} + \underbrace{\sum_{m=1}^{N} W_{nm}\chi_m \left[V_m\left(t-\frac{d_{nm}}{v}\right)\right]}_{\text{Connections}} + \underbrace{B_{t,n}\cdot\Omega_{t,n}}_{\text{Noise}} \quad (1)$$

where

- dt is a formal infinitesimal time step,
- $\tau \in \mathbb{R}_+$ is the leaky time (or characteristic time of the membrane (Gerstner and Kistler 2002)),
- $\chi_n[V_n(t)]$ is, for the neuron n, the indicator function of the set of potentials bigger or equal to V_n^*. Namely, $\chi_n[V_n(t)] = 1$ whenever $V_n(t) \geq V_n^*$ and $\chi_n[V_n(t)] = 0$ otherwise. The distribution of all the characteristic membrane potential firing threshold is approximately[4] Gaussian with a probability density function close (see footnote 4) to $h(V^*) = \frac{1}{\Delta V^* \sqrt{2\pi}} e^{-\frac{(V^*-1)^2}{2\Delta V^{*2}}}$ where ΔV^*, the standard deviation, is a parameter,
- $d_{nm} = d_{mn}$ is the distance between the neuron n and the neuron m. In the experiments related in Eckmann et al. (2008), one finds a 2D density of about 2,000 $\frac{\text{cells}}{\text{mm}^2}$. This leads us here to fix the metric scale in our simulations: If we observe an expected mean number of neurons of 2,000 neurons inside the grid square, we assume that this square measures 1 mm^2. Nevertheless, we can also measure the distance in an arbitrary unit given by the expected number of neurons in a row but we need the metric scale to compare our signal propagation velocity to the experimental one,
- v is the propagation velocity of the signal in the neural network,
- $B_{t,n}$ is, for each time t and each neuron n, a Gaussian random variable with mean $\sigma > 0$ and standard deviation $\frac{\sigma}{3}$. Without addition of noise, all the membrane potentials of our simulations will tend to 0 (because of the leaky time). To avoid that, we add Gaussian noise to each neuron n. The choice of $B_{t,n} \sim \mathcal{N}\left(\sigma, \frac{\sigma}{3}\right)$ (for all n and for all $t > 0$) guarantees that the noise we add is a positive quantity between 0 and 2σ (99% of the times). To generate this Gaussian noise, we use a Box–Muller transform. In Section 4.1, we will explain how to fix the parameter σ.
- $\Omega_{t,n}$ is a Markovian exponential clock with a mean rate ω. In Section 4.1, we will explain how to fix the parameter ω. Concerning the Markovian exponential clock, for most t, one has $\Omega_{t,n} = 0$, but sometimes $\Omega_{t,n} = 1$. More precisely, the distribution of the time intervals Δt of the continuous set t where $\Omega_{t,n} = 0$ follows the exponential distribution $\frac{1}{\omega} e^{-\frac{\Delta t}{\omega}}$ (ω is the mean value). Finally, it means that $B_{t,n} \cdot \Omega_{t,n}$ is a noise $B_{t,n}$ which acts on the membrane potential of neuron n only when the exponential clock $\Omega_{t,n}$ rings.

By looking at Eq. (1), we see that, in principle, we can compute every membrane potential all the time. But it is not useful and too complicated to compute every membrane potential continuously. Choosing a fixed time step $\delta t > 0$ also introduces some problems like synchronized events and systematic errors (Cessac and Samuelides 2007). In the program, made in Perl, we compute the membrane potential only when an event happens.[5] At this time, we check if the neuron fires or not. So, in the program, we store the events to find out the next membrane potential to update. In other

[3] We know that the membrane potential fluctuates more or less between −70 and −50 mV (Gerstner and Kistler 2002). But to simplify, we will approximately scale the membrane potential between 0 and 1.

[4] We decided that negative membrane potential firing thresholds are not allowed since we do not want the firing condition $(V_n(t) > V_n^*)$ to be reached for some neurons each time they are reset.

[5] Here, by event we mean the moment when a neuron receives a signal from another neuron or when a neuron receives some noise (i.e., the Markovian exponential clock $\Omega_{t,n}$ rings).

words, our simulations (Eq. (1)) are event-based simulations. The firing time of neurons is not discretized but computed event per event at the machine precision level. This way of doing provides, in principle, unbiased simulations (Cessac et al. 2008; Cessac and Samuelides 2007; Rudolph and Destexhe 2007). Since the time is not discretized, the noise is not added to every neuron at the same moment. The exponential clock which is a natural way to split the events in time (e.g., radioactive decay follows an exponential law), guarantees that on average a neuron receives noise as often as another neuron and that the strategy is not clock-driven. Remark that Eq. (1) is written as if the time is discretized only to simplify the reading.

Note that if "every" neuron fires at (almost) the same time (this may happen in a burst) then all the membrane potentials are reset to 0 at the same time; the neurons are synchronized. To avoid that this situation occurs too often, when we initialize a sequence, we give to each neuron n a membrane potential in $[0,\ V_n^*)$ (uniformly distributed). Note that we reinitiate a sequence each time a burst is too long, so it is possible that during a simulation the neurons get synchronized. The reinitiation of sequences does not occur very often (less than one time every thousand bursts). These reinitiations have two main reasons. (1) Reinitiation implies that we choose other initial conditions and run our simulation again. The invariance of our results under the change of initial conditions is then ensured by the reinitiation of sequences. We did not remark any sensitivity to initial conditions in any results we present in this paper. (2) If a burst is too long, the reinitiation of sequences allows to focus again on the neurons that fire early in the bursts and not to compute bursts evolution.

Note also that if the mean exponential clock rate ω is too small relatively to the leaky time τ, it does not really matter which kind of distribution we use for the noise $B_{t,n}$. This means that if $\omega \ll \tau$ then we can use $B_{t,n} = \sigma$ for all t and for all n as the noise distribution $B_{t,n}$ and the result of the simulations remains the same.

2.2 Values of parameters and simulation choices

The parameters are fixed in a way to observe activity like the one observed in the experiments (Eckmann et al. 2008) when we restrict the observation to sixty neurons. This section provides a list of the order of magnitude of the parameters used in Eq. (1). Note that the reader can find almost all the information in Eckmann et al. (2007).

- We made simulations for different sizes $N \in \mathbb{N}$. But beyond $N \sim 4$ it does not affect the presence of bursts and leaders. This means that we already get a leader when we consider only four neurons. All the figures presented in this paper show simulations with $N = 900$; The reason is only plot convenience. During the study, we have tested our results for simulation size between $N = 4$ to $N = 40{,}000$.
- In fact fixing the dentrites size r, the mean axon length L and the axon length distribution fix the distribution function for the sons (out-degree) and the mean number of connections per neuron (noted $\langle$connections/neuron$\rangle$). Remark that the number of sons per neuron distribution looks like the axon length distribution while the number of fathers per neuron distribution is always approximately Gaussian distributed (data not shown). Note also that the geometry we have chosen for our simulations induces that the successful pre-burst shows locality, like the one observed by the authors in Eckmann et al. (2008). Finally in most of our simulations, we have chosen $\mathsf{r} = 0.85$ and $L = 7$, then $\langle$connections/neuron$\rangle \cong 11$.
- The synaptic weight w is surely a function of the neuron and of the time (the neuron's learning). As soon as we choose a mean number of connections per neuron and considering the kind of neural activity we want, we can fix w. We use $\mathsf{w} \sim \frac{1}{10}$. Note that if $\mathsf{w} \cong \langle V^* \rangle = 1$ (where $\langle V^* \rangle$ is the mean of all the neuron membrane potential firing thresholds) then all neurons are too strongly correlated and if $\mathsf{w} = 0$ then all neurons are independent.
- For the inhibitory proportion r, the choice of $r = 0.2$ is reasonable. Depending on the neural culture type, the inhibitory cells proportion can change approximately from 20 to 30% (see Soriano et al. 2008).
- In our simulations, the leaky time τ is about 100 ms. Note that the order of magnitude is the correct one (Alvarez-Lacalle and Moses 2007). To be exact we compute with $\tau = 0.1$ s, this means that the used time unit is the second.
- The propagation speed v in a neural network is between 50 and 100 $\frac{\text{mm}}{\text{s}}$, see Eckmann et al. (2007). In our case, v should be replaced by the propagation speed in the axon which is bigger. However, we have decided to use this range throughout.
- The standard deviation of the membrane potential firing threshold ΔV^* is also a parameter. We used $0 \leq \Delta V^* \leq 0.2\langle V^* \rangle$, which guarantees that neurons are quit similar and still the membrane potentials do not get synchronized too often.
- For the exponential clock rate we use ω between 0.001 and 0.01 s.

Table 1 Known and unknown parameters of the simulations

The unknown parameters will be set in Section 4.1

	Neural network parameters	Dynamical parameters
Known	$r \cong 20\%$ (inhibitory proportion)	$\tau \cong 100$ ms (leaky time)
	r, L, (mean number of connections)	$v \cong 100 \frac{\text{mm}}{\text{s}}$ (propagation speed)
To be set	N (computing-memory)	$\langle V^* \rangle - \overline{V} > \mathsf{w} > 0$ (synaptic weight)
	ΔV^* (firing threshold standard deviation)	σ, ω (noise parameters)

- The mean noise σ is determined by the kind of neural activity we want to have (observe). If there is too much noise then we loose the locality in the successful pre-burst because we have a lot of uncorrelated activities. Note that the mean membrane potential (without connection) $\overline{V} = \lim_{T\to\infty} \frac{1}{T} \int_0^T V(\tilde{t})\, d\tilde{t}$ is about[6] $\frac{\tau\sigma}{\omega}$. We want the mean membrane potential $\overline{V}$ to be high enough to get some neural activity due to the noise. But we also want that $\overline{V} + \mathsf{w} < \langle V^* \rangle$, so that one spike does not necessarily create a burst.
  One might think that to keep the neural activity one can vary the values ω and σ, keeping the ratio $\frac{\sigma}{\omega}$ constant, because the mean membrane potential $\overline{V}$ is about $\frac{\tau\sigma}{\omega}$. But to preserve the neural activity, the mean membrane potential $\overline{V}$ is not that relevant. However, it is necessary to keep constant the mean time the membrane potential of neurons need to reach the value V^*. From this point of view the relation between σ, ω and w is a first passage time problem. Note also that if the value of the mean membrane potential $\overline{V}$ is too low then there is no neural activity due to the noise (this means no neural activity at all). To conclude, even if the exact value of the mean membrane potential $\overline{V}$ is not fundamental, this value must not be too far from the mean of all neurons membrane potential firing threshold $\langle V^* \rangle$ (see Gerstner and Kistler 2002).

The parameters N, r, L, ΔV^* and r are the neural network parameters and the parameters τ, v, w, σ and ω are the dynamical parameters (Table 1).

3 General appearance of the simulations and some definitions

In this section we show what is the product of our simulations and we give the definitions of what we call a leader neuron, according to Eckmann et al. (2008).

3.1 General appearance

Like in the experiments (Eytan and Marom 2006; Eckmann et al. 2008; Wagenaar et al. 2006a), we want to look at the neural activity. The output of our simulations consists of a list of ordered spikes times. For each spike i, the list gives us t_i, the time of the ith spike, and n_i, the neuron that fired. Then, considering only the spike chronology, we analyze the "spike sequence" of a subset (or all) neurons of our simulations.

3.2 Definitions

Figure 2 represents a part of a simulation and leads us to define sequences in the simulations. This section is roughly the same than Eckmann et al. (2008, Section 2.3). Precisely we will define mathematically what we call a burst and a leader. In order to make the present paper comparable to Eckmann et al. (2008), we adhere strictly to the same definitions. So the reader who has read Eckmann et al. (2008) or knows these definitions can skip this part and move directly to the next section.

3.2.1 Definition of bursts and their triggers

First we divide all the spikes of our list into four classes: *burst*, *successful pre-burst*, *aborted pre-burst*, *isolated spike*, and each spike belonging to one and only one class. The precise definitions are given below, but basically a spike is in a burst if it is in a group of many spikes that follow each other closely. If a spike is not in a burst it can be in a successful pre-burst or aborted pre-burst. But it must be anyway in a sequence of spikes that are close enough in time so that communication between them is still possible. The distinction between successful or aborted pre-burst depends on whether the spike sequence is eventually followed by a burst or not. Finally, all other spikes are isolated.

More precisely, we use three parameters, n_{burst}, δt_{burst}, and $\delta t_{\text{isolate}}$. We first look for interspike gaps of length at least $\delta t_{\text{isolate}}$, and we divide the set of all spikes into disjoint subsets $\mathcal{R}_k$ of consecutive spikes, where k is a running index. The $\mathcal{R}_k$ have the property that if (the spike) i and $i+1$ are in $\mathcal{R}_k$ then $t_{i+1} - t_i \le \delta t_{\text{isolate}}$, while if $i \in \mathcal{R}_k$ and $i+1 \in \mathcal{R}_{k+1}$ then $t_{i+1} - t_i > \delta t_{\text{isolate}}$. The

[6] The mean membrane potential charge due to the noise is $\sigma + \sigma e^{-\frac{\omega}{\tau}} + \sigma e^{-2\frac{\omega}{\tau}} + \ldots = \frac{\sigma}{1-e^{-\frac{\omega}{\tau}}} \cong \frac{\tau\sigma}{\omega}$ if $\frac{\omega}{\tau}$ is small.

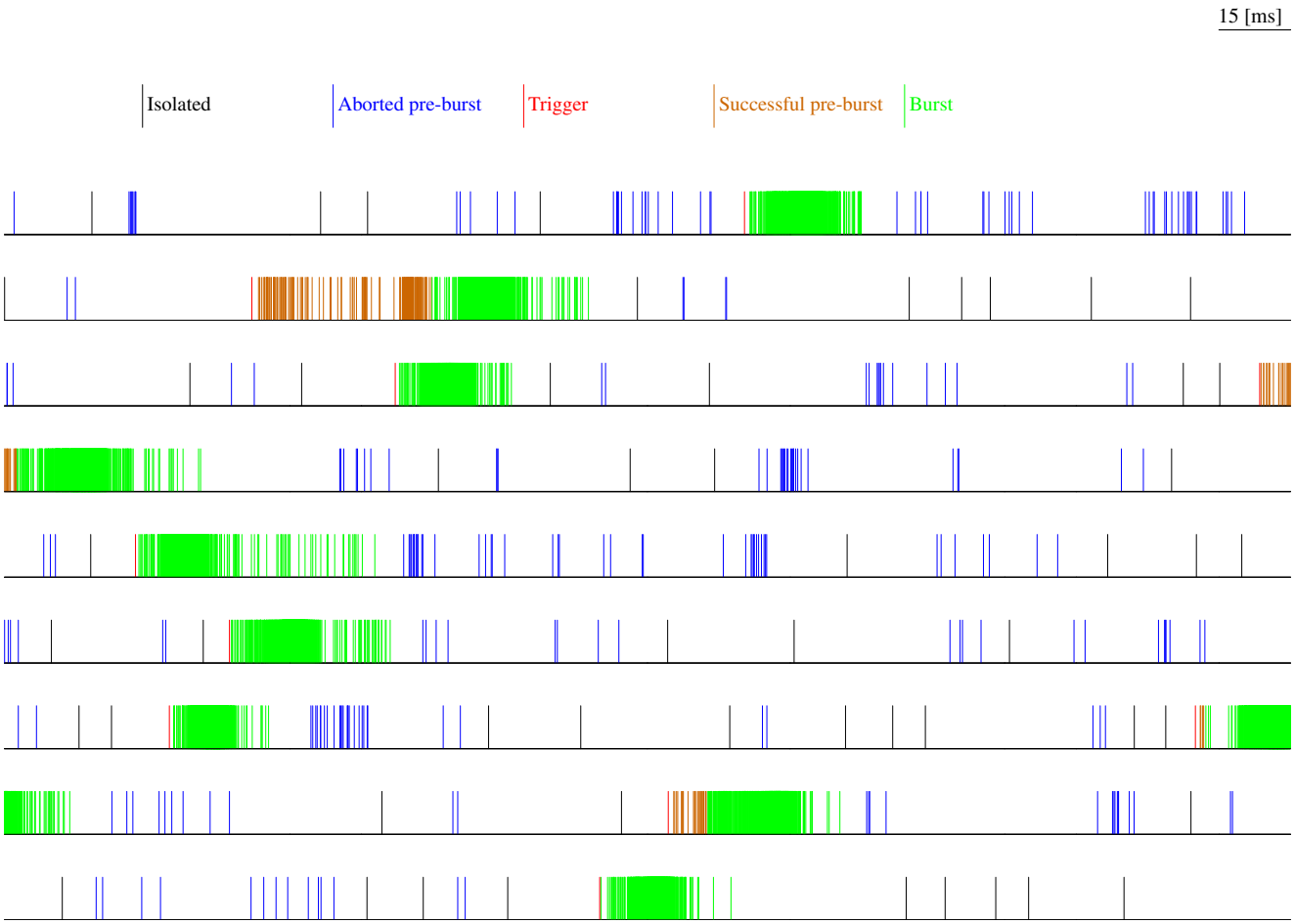

Fig. 2 Picture of the temporal evolution of a simulation for the whole neural activity. This time diagram is a direct representation of the data obtained with our simulations where all spikes are represented without specification of which neuron is firing. Precisely, in this figure, the time goes from the left to the right and from the top to the last row. Every *vertical bar* represents a spike. Parameters: $N = 900, \mathsf{r} = 0.85, L = 7, r = 0.2, \Delta V^* = 0.05, v = 5\frac{1}{\text{ms}}$, $\mathsf{w} = 0.1$, $\tau = 100$ ms, $\sigma = 0.008$, $\omega = 0.001$ s, $n_{\text{burst}} = 500$, $\delta t_{\text{burst}} = 15$ ms and $\delta t_{\text{isolated}} = 5$ ms. The color code, that gives a representation of the different definitions explained in the following section, is the following: black for *isolated spike*, blue for *aborted pre-burst*, red for *trigger*, brown for *successful pre-burst*, and green for *burst*

rationale is that if the interspike gap is so large that the spike $i+1$ is due to noise and not to the axon signaling of the precedent (in time) spike i (i.e., if $t_{i+1} - t_i > \delta t_{\text{isolate}}$ then the spikes belong to separate subsets).

We now want to further divide each $\mathcal{R}_k$ into the burst itself, characterized by a high density of spikes, and its precursor which immediately precedes it in time but has a lower density. Each of the $\mathcal{R}_k$ contains at least one spike, but may contain many. In each $\mathcal{R}_k$ we first look for a spike that is followed by at least $n_{\text{burst}} - 1$ spikes in $\mathcal{R}_k$ within a lapse of time δt_{burst}. Denoting this spike's index by $i_* = i_*(k)$, this is the first index in $\mathcal{R}_k$ with the property:

$$t_{i_*+n_{\text{burst}}-1} - t_{i_*} < \delta t_{\text{burst}} \ . \tag{2}$$

If the condition (2) is met then we subdivide $\mathcal{R}_k$ into two disjoint sets at i_*: $\mathcal{R}_k = \mathcal{P}_k \cup \mathcal{B}_k$ ($\mathcal{P}_k$ can be empty). The index i_* up to the last index in $\mathcal{R}_k$ make up the burst $\mathcal{B}_k$. The letter $\mathcal{P}$ refers to successful pre-bursts and $\mathcal{B}$ refers to bursts.

If the condition (2) is never met in $\mathcal{R}_k$, then the set $\mathcal{R}_k$ is not subdivided. This is called an *aborted pre-burst* if it has more than one spike and is an *isolated spike* otherwise.

For these k where such an i_* can be found, we check if it is also the first spike in $\mathcal{R}_k$. If so, this burst is an *immediate burst* that has no successful pre-burst, so that $\mathcal{R}_k = \mathcal{B}_k$. For all the other bursts we divide $\mathcal{R}_k = \mathcal{P}_k \cup \mathcal{B}_k$ where $\mathcal{P}_k$ are the index $i \in \mathcal{R}_k$ with $i < i_*$, and $\mathcal{B}_k$ are the others.

Between bursts the neural activity is much lower, and we label these periods as *quiet*. Each quiet period, denoted $\mathcal{Q}_b$, for a running index b, is actually a concatenation of consecutive $\mathcal{R}_k$'s that did not contain a

Table 2 Burst detection parameters

Analyzed neurons	n_{burst}	δt_{burst} (ms)	$\delta t_{\text{isolate}}$
60	20	$\frac{\sqrt{N}}{2}$	$\frac{\text{max axon length}}{v}$
N	$\gtrsim \frac{N}{10}$		

burst in the earlier stage, or else an empty set. We now renumber the set of index as follows

$$\{1, \ldots, M\} = \mathcal{Q}_1 \cup \mathcal{P}_1 \cup \mathcal{B}_1 \cup \mathcal{Q}_2 \cup \mathcal{P}_2 \cup \mathcal{B}_2 \cup \ldots ,$$

with $\mathcal{B}_b$ the b'th burst, $\mathcal{P}_b$ the corresponding successful pre-burst (if it exists else $\mathcal{P}_b$ is empty) and $\mathcal{Q}_b$ the corresponding quiet phase. We define the *trigger* of burst b as the neuron n_{i_b}, where i_b is the index of the first spike in $\mathcal{P}_b$ (resp. $\mathcal{B}_b$ if $\mathcal{P}_b$ is empty like for an immediate burst).

The parameters n_{burst}, δt_{burst}, and $\delta t_{\text{isolate}}$ that we used are shown in Table 2. Remark also that the time parameters $\delta t_{\text{isolate}}$ and δt_{burst} have to be smaller than the characteristic time of the membrane τ. The rationale for these choices are: Firstly, to cross the distance of the biggest possible axon, the signal, at the velocity v, needs a time of $\frac{\text{max axon length}}{v}$. This computation gives us the order of $\delta t_{\text{isolate}}$. This means that only the signaling velocity is taken into account to compute $\delta t_{\text{isolate}}$. Secondly, even in a burst, the neural activity is not regular. Thus, to balance this effect we need δt_{burst} to be high enough. Finally, for n_{burst} we want it high enough to guarantee that a burst includes many neurons (typically $n_{\text{burst}} \gtrsim N/10$).

3.2.2 Leaders

For every successful pre-burst, aborted pre-burst or immediate burst, the neuron which fires first is called the *trigger*. Since we are interested in their special rôle, we first need to make sure that triggers are not just neurons with high neural activity, which are statistically more often the first ones to fire. The following discussion will exhibit that leaders are over-proportionally more often triggers.

To qualify a neuron as a leader, we require that a trigger's probability to lead bursts should be significantly higher than its probability to fire. Let M be the total number of bursts in a simulation. For each neuron n, we define a_n as the number of times that neuron n has spiked during the simulation. Now, let us consider a spike, and term by q_n the probability[7] that neuron n has fired that spike: $q_n = a_n / \sum_{n'} a_{n'}$. The probability for the neuron n to be a spurious, or random trigger F times in M bursts is given approximately[8] by the binomial distribution $P_n(F)$:

$$\binom{M}{F} q_n^F (1 - q_n)^{M-F} . \tag{3}$$

In the limit of large M and reasonable q_n this distribution is approximated by a Gaussian of mean Mq_n and variance $Mq_n(1 - q_n)$. On the other hand, we denote by f_n the actual number of bursts that neuron n leads (note that $\sum_n f_n = M$).

Thus we have a scale on which to test triggering. We define α_n, a "leadership score", and decide that a neuron is a *leader* if it scores at least three standard deviations above the natural expectation value. The criterion for the leadership of neuron n is therefore

$$\alpha_n = \frac{f_n - Mq_n}{\sqrt{Mq_n(1 - q_n)}} > 3 . \tag{4}$$

Because we expect $\alpha \sim \mathcal{N}(0, 1)$ to be Gaussian, Eq. (4) corresponds to a p-value of 0.001.

4 Results

In this section we explain our results. We prove that our simulations have stable leaders and we identify the topological properties of these leaders. An analysis of the first to fire neurons exhibits that the leader properties we find are the correct ones.

4.1 About the parameters and some statistics

The next step consists in analyzing our simulations knowing that our results will be more consistent if we span as many parameters as possible. However, our goal is not to obtain a phase transition diagram (Naud et al. 2008), so we are not going to vary all parameters (most of the them were fixed in Section 2.2 through Table 1). Some parameters have not been fixed yet, including dynamical parameters like w, σ and ω. So we still have to find (and fix) a range for the parameters

[7] Unbiased estimator of the considered probability.

[8] It would be exactly the binomial distribution if all the spikes were independent. All the spikes are certainly not independent because neurons are connected. So the binomial distribution is not the correct one but gives a good enough approximation (see Zbinden 2010).

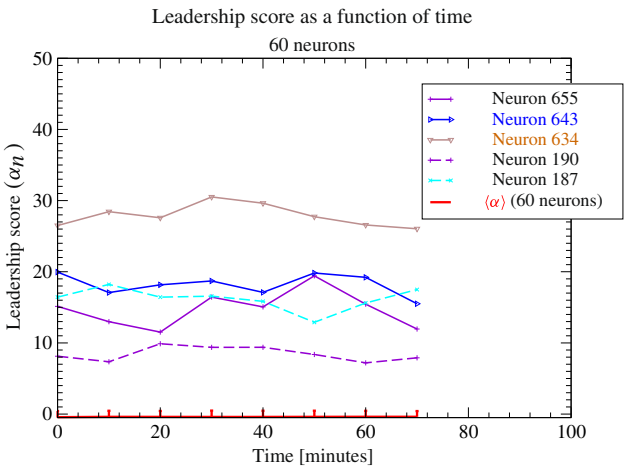

(a) The leadership score when we look at only 60 neurons like in the experiments. We see that we have leaders and even very good ones. We also see that the average leadership score $\langle\alpha\rangle$ is about 0. Note that in this graph, each point represents 600 seconds of simulation that contains more than 2500 bursts. Remark that the best leader among 60 neurons is not necessarily a leaderwhile we consider all the neurons (see Figure 3(b)). In the restricted case, the neurons detected as leaders can be first to fire neurons (see Section 4.4).

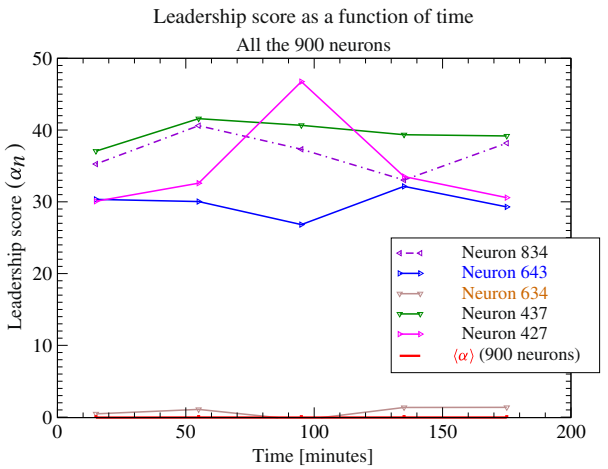

(b) The leadership score when we consider all the 900 neurons. We can say that these neurons are the "true" best leaders of the simulation. Note also that, luckily, one of the best leaders was in the 60 selected neurons. But even when it is not the case, when we consider only 60 neurons, some neurons show very good leadership scores. On this graph, each point represents about 2000 seconds of simulation that contains more than 8800 bursts.

Fig. 3 Leadership score of a few neurons for the simulation shown in Fig. 2. Note that the leadership score depends on the number of neurons considered for the analysis (see neurons 634, 643 and Section 4.4)

ΔV^*, w, σ and ω in a way to obtain "reasonable"[9] parameters for our simulations which involves distinguishing bursts, successful pre-bursts and quiet periods. One of the best ways to do that mathematically is to look at the time interspike distribution (TID) and compare with the experimental one (data not shown). Note that to distinguish bursts and quiet periods, the TID must have a kind of (long) tail (since most of the spikes are in bursts but some have to be outside). This means that comparing the experimental TID and the simulated TID result in comparing the tail of these distributions. Finally showing the full TID is not really the proposal of this paper (the tail comparison is done in Zbinden 2010). The analysis of the membrane potential profile and the time length distribution are also possible in the simulations (see Zbinden 2010).

In our model, the exact value of ω does not really matter, since the leaky time τ fixes the time unit. Therefore, only the ratio between ω and τ matters. In the specific case $\omega > \tau$, not studied in this paper, the leaky integrate and fire model will be replaced by a simpler model (Eckmann et al. 2010) in which the definition of leaders has to be modified as well.

4.2 Existence of leaders

In Section 3.2.2, we defined, for every neuron n a leadership score α_n (see Eq. (4)) that compares the triggering frequency to the leadership expected frequency (computed with respect to the neural activity frequency). Figure 3 show the leadership score as a function of the time for a few neurons. In these figures we see that our simulations have stable leaders. Note that this result is very robust. We mean that the choice of the used parameters in simulations is not important. As soon as we use "reasonable" (see footnote 9) parameters, our simulations have leaders. This is still true when we only look at a few neurons instead of all of them (Fig. 3(a)). Even more, we can change the axon length distribution and the simulations still have stable leaders.

Note also that even a random network with a uniform probability of connections[10] shows bursts and

[9]Here by "reasonable" parameters, we mean to observe a neural activity more or less like the one in Fig. 2 but without a precise predicting spike timing (Brette and Gerstner 2005; Luscher et al. 2006). This means that we want to observe quiet periods, successful pre-bursts and bursts in a way to find leaders. Note that this range of "reasonable" parameters is quite large and the relation between the dynamical parameters is non trivial, see remark in Sections 2.2 and 4.1.

[10]This means a random network in which the probability of connections between all possible pairs of neurons is equal.

stable leaders but, in this case, we do not observe any spatial locality (unlike in the experiments (Eckmann et al. 2008)). During our investigations, we tested also homogeneous networks. By homogeneous networks, we mean networks in which all neurons have exactly the same number of connections (for example the eight nearest neighbors). In these kind of networks, one of the differences between neurons is the number of inhibitory sons and fathers and this suffices to observe stable leaders (Zbinden 2010). To summarize, the network topology does not really matter since we observe stable leaders as soon as the number of neurons N is much higher than the mean number of connections per neuron.

In our simulations, with $N > 400$ about 5–10% of the neurons have a mean leadership score (Eq. (4)) bigger than the threshold 3 when we consider all the neurons. While considering only 60 neurons, about 15% neurons have a mean leadership score bigger than the threshold 3. Also note that even if the leadership score can fluctuate during the simulations, its mean value stays stable (i.e., its standard deviation is small). Of course, the leader ratio decreases when the mean noise σ increases. This fact is logical because in a too noisy neural activity it becomes more difficult to identify the trigger of each burst. Note also that it seems that when ΔV^* (standard deviation of the membrane potential firing threshold) is between 0.05 and 0.1 the leader ratio seems maximal (data not shown).

In the experiments (Eckmann et al. 2008), one electrode captures in general the spike signal of several neurons (Eckmann et al. 2008, Fig. 1a). But, in our simulations, up to this point we considered each neuron separately, as if one electrode measures only one neuron. Remark that the leadership score of groups of neurons also reach the value 3 for some groups (Zbinden 2010).

Moreover, we have tested the effect of other synaptic weight distributions on the presence of leaders and the conclusion is that stable leaders still exist.

One can ask: Do leaders still exist in a given simulation if we remove the observed leaders? The answer is yes. Precisely, in Section 4.3.2 we discuss the combination of properties that a neuron needs to be a leader. The conclusion is that neurons with properties near the typical leader properties are the leaders. When we remove these leaders, then other neurons have their properties near the typical leader properties and become leaders (typically the followers if we dress a list). Finally, a neuron is a leader because of its particular connections in the network and its own properties (see discussion at the end of Section 4.3.2).

At this point, our simulations reproduce basically all the findings of Eckmann et al. (2008) (presence of leaders, signature of bursts, force of leaders,...); see Zbinden (2010). The advantage of simulations is that we have access to a lot of details that we did not have access to in the experiments and we can analyze the topology of the network to find out the properties of leaders.

4.3 Leader properties

4.3.1 Some facts about the leader properties

In Figs. 4 and 5 we clearly see that the leaders seem to have some special properties compared to the other neurons. More precisely, Fig. 4(a) shows that good leaders typically have a low membrane potential firing threshold. This fact exhibits that to be a good leader, a neuron must have the property of firing early. But, this property is not the only one a neuron needs to have to be a leader. Indeed the best leader in Fig. 4(a) is not the neuron with the lowest membrane potential firing threshold. Thus, another property of the leaders is easy to highlight: the leaders are excitatory neurons[11] (see Fig. 5(a)). Figure 5(b) also gives an idea of another typical leader property. Indeed, good leaders seem to have only a few excitatory fathers. This means that to be a leader, a neuron should not be the follower of another excitatory neuron. Finally, in Fig. 4(b), we see, as in Eckmann et al. (2008), that better leaders trigger more bursts.

We can also look at the leadership score compared to the neural activity ratio of the neurons shown in Fig. 6. Firstly, remember that to compute the leadership score we use the neural activity ratio q (see Eq. (4)). Secondly, look at Fig. 6 and remark that there are as much leaders with a high neural activity ratio as leaders with a low neural activity ratio. So, clearly and as expected, for a given neuron there is no link between having a high leadership score and the neural activity

[11] Remark that in the special case where $\omega \ll \tau$, we rarely observed a few inhibitory neurons with a leadership score higher than 3. This can happen only when these inhibitory neurons have a very low membrane potential firing threshold, a few excitatory fathers and a lot of inhibitory fathers. The reason is as follow, because $\omega \ll \tau$, the network gets synchronized after the first burst and these particular inhibitors have the faculty to fire even before the true trigger of the burst. Beside the type of their fathers implies a very low neural activity, so their leadership scores are potentially good. Note that the few best leaders are always excitatory neurons.

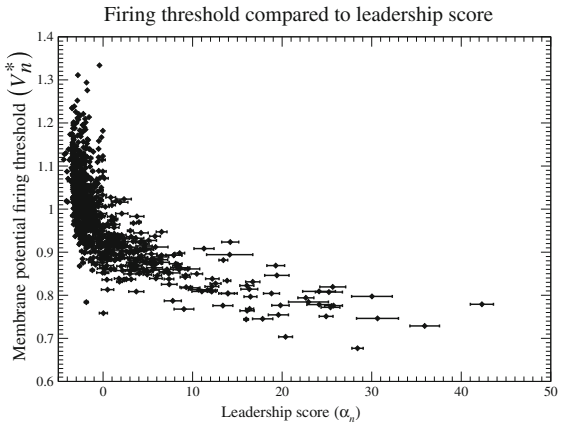

(a) The membrane potential firing threshold (V_n^*) compared to the leadership score (α_n). We see that good leaders have a low membrane potential firing threshold ($\langle V^* \rangle = 1$).

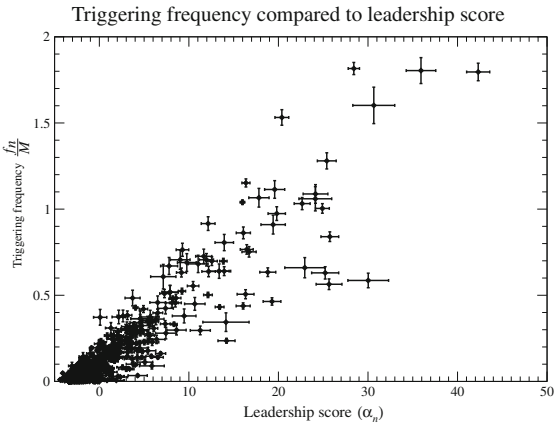

(b) The triggering frequency (f_n/M) compared to the leadership score (α_n). These two things are mostly proportional.

Fig. 4 Some properties of leaders for simulations with parameters close to the one we showed in Fig. 2. Note that each point in these figures represents an average of the results for five simulations using the same neural network and the same parameters. Each simulation contains more than 10,000 bursts and the simulated time was longer than 25 min. Parameters: $N = 900$, $\mathsf{r} = 0.85$, $L = 7$, $r = 0.2$, $\Delta V^* = 0.1$, $v = 5\ \frac{1}{\text{ms}}$, $\mathsf{w} = 0.1$, $\tau = 100$ ms, $\sigma = 0.008$, $\omega = 0.001$ s, $n_{\text{burst}} = 100$, $\delta t_{\text{burst}} = 15$ ms and $\delta t_{\text{isolated}} = 5$ ms

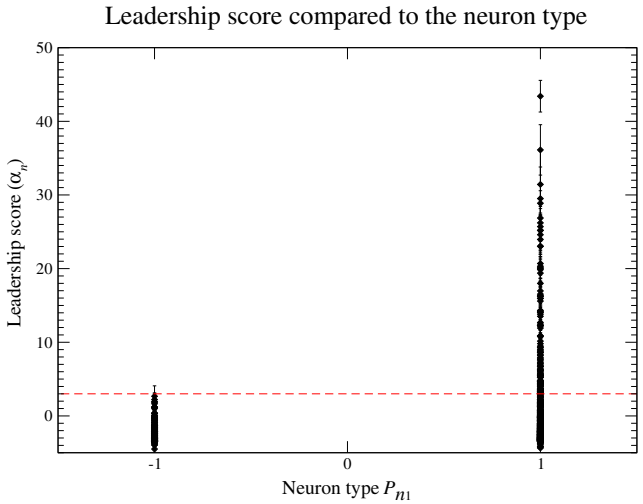

(a) The leadership score (α_n) compared to the neuron type (P_{n1}). The *red dashed line* separates leaders and non-leaders. This figure shows clearly that leaders are excitatory neurons (+1).

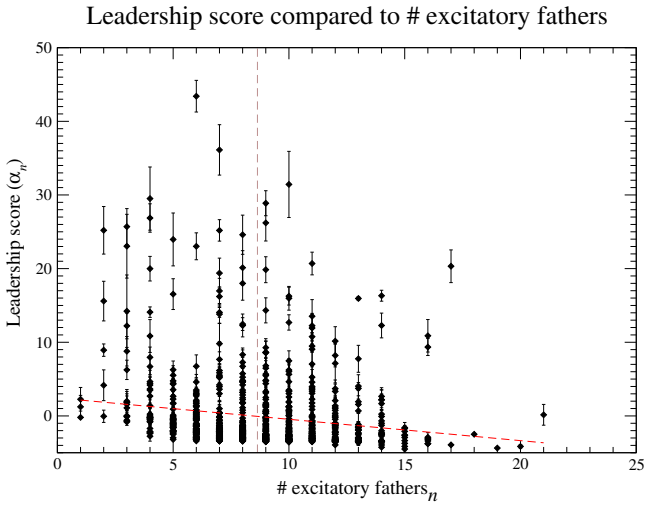

(b) The leadership score (α_n) compared to the number of excitatory fathers. The *red dashed line* is a linear regression with correlation $r^2 \cong -0.29$ that shows that, on average, a higher number of excitatory fathers implies a lower leadership score. The mean number of excitatory fathers per neuron is represented by the *brown dashed line*.

Fig. 5 Illustration of importance of the number of excitatory fathers and of the type of neurons in the leadership score. As for Fig. 4, the error bars of each point in this figure are computed using five simulations done with the same network and parameters. The parameters are the same as in Fig. 4: $N = 900$, $\mathsf{r} = 0.85$, $L = 7$, $r = 0.2$, $\Delta V^* = 0.1$, $v = 5\ \frac{1}{\text{ms}}$, $\mathsf{w} = 0.1$, $\tau = 100$ ms, $\sigma = 0.008$, $\omega = 0.001$ s, $n_{\text{burst}} = 100$, $\delta t_{\text{burst}} = 15$ ms and $\delta t_{\text{isolated}} = 5$ ms

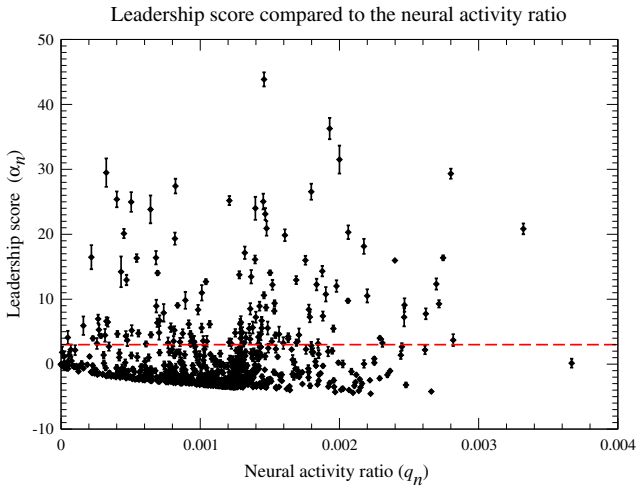

Fig. 6 The leadership score (α) compared to the neural activity ratio (q). The *red dashed line* separates leaders and non-leaders. With these specific parameters, the leaders are distributed more or less fairly around $\bar{q} = \frac{1}{N} \cong 0.0011$ even if the non-leaders seem to accumulate on a line. Note that, as before, each point in this figure represents an average of the results for 5 simulations using the same neural network. Parameters: $N = 900$, $\mathsf{r} = 0.85$, $L = 7$, $r = 0.2$, $\Delta V^* = 0.1$, $\upsilon = 5\ \frac{1}{\text{ms}}$, $\tau = 100$ ms, $\mathsf{w} = 0.1$, $\sigma = 0.008$, $\omega = 0.001$ s, $n_{\text{burst}} = 100$, $\delta t_{\text{burst}} = 15$ ms and $\delta t_{\text{isolate}} = 5$ ms

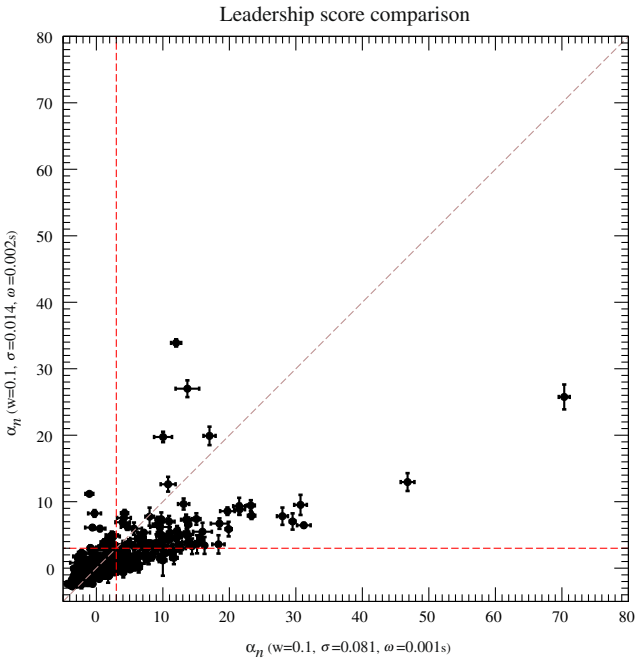

Fig. 7 The leadership score α_n of two different simulations using the same neural network. The *red dashed lines* separate leaders and non-leaders for both simulations. We observe that the best leader is not necessarily the same and some neurons are leaders with a set of parameters but are not leaders with the other set. We also observe that most of the time a good leader continues being a good leader in both simulations. Like for Fig. 4, the error bars are computed by averaging over five simulations using the same network and dynamical parameters w, σ and ω. Common parameters: $N = 900$, $\mathsf{r} = 0.85$, $L = 7$, $r = 0.2$, $\Delta V^* = 0.1$, $\upsilon = 5\ \frac{1}{\text{ms}}$, $\tau = 100$ ms, $n_{\text{burst}} = 100$, $\delta t_{\text{burst}} = 15$ ms and $\delta t_{\text{isolate}} = 5$ ms

ratio, even if a good leader triggers a lot of bursts (see Fig. 4(b)).

Before trying to find more leader properties, we add more remarks about Fig. 6. We note that there exist some neurons with a very high positive leadership score ($\alpha > 10$) but there is no neuron with a very low leadership score ($\alpha < -10$).

The mean neural activity ratio[12] noted $\bar{q}$ is always equal to $1/N$. Figure 6 in which $\bar{q} = \frac{1}{900} \cong 0.0011$ as expected, illustrates this fact. However, the standard deviation of the neural activity ratio distribution depends strongly on the standard deviation of the membrane potential firing threshold ΔV^*. This can be understood easily since the neural activity ratio of a neuron depends on the number of fathers of this neuron and on its membrane potential firing threshold. Figure 6 in which $\Delta V^* = 0.1$, is more or less an illustration of the neural activity ratio distribution.

All the relations between a property and the leadership score that we showed did not exhibit an as good link as the relations shown in Figs. 4(a) and 5(a). We can also note another important fact: In the special case where we use a network with every membrane potential firing threshold fixed to $\langle V^* \rangle$ (i.e., $\Delta V^* = 0$) or/and without inhibitory neurons (i.e., $r = 0$), our simulations still have stable leaders. These two facts lead us to the following hypothesis: being a leader results from a non trivial combination of properties.

To find these properties, we perform the following experiment: We take a given network[13] and make several simulations with this network but change some of the dynamical parameters (τ, υ, w, σ and ω) in a way of keeping a "reasonable" (see footnote 9) simulation. Then, we compute the leadership score of each neuron and we do this for each simulation. As a result, we find that the best leader is not always the same even if most of the time a leader stays leader. Figure 7 illustrates this fact and this forces us to admit that the leader properties depend on the dynamical parameters. Nevertheless, we can probably find a trend of the properties of a typical leader by doing a linear least squares analysis for all our simulations. Indeed, in Fig. 7 more than

[12]The neural activity ratio of neuron n, noted q_n, is defined in Section 3.2.2.

[13]This means that we choose N, r, L, p, ΔV^*, r and build a realization of a network (i.e., W and V_n^* are known for all n).

90% of the leaders continue being leaders and non leaders continue being non leaders under the change of dynamical parameters. Moreover, the leader properties that we are looking for are topological properties, which means mainly neuron and network properties. Thus, the neural activity ratio q and the dynamical parameters will not be taken into account when we will be searching for the leader properties since our aim is to forecast which neurons will be leaders, before we run our simulation.

Before going through this linear least squares analysis, note that in the experiments related in Eckmann et al. (2008), the leaders change during the days spent *in vitro* with a typical life time of about one day (see Eckmann et al. 2008, Fig. 3a). While, in the simulations, the leaders stay the same in a given network if we do not change the dynamical parameters of the simulation. So, one of the interesting facts in the simulations is that to change the leaders we do not need to change the network, some changes in the dynamical parameters are enough (we consider the synaptic weight w as a dynamical parameter).

4.3.2 Finding the leader properties

To find out the leader properties we do the following linear least squares analysis. First, we build a vector $\vec{\alpha} = \{\alpha_n\}_{n=1,\dots,N}$ that contains the leadership score α_n of each neuron n of a given simulation. Then we construct a matrix $P = \{P_{ni}\}_{1\le n\le N,\ 1\le i\le 6}$ that contains all the neuron properties (excitatory or inhibitory neuron and membrane potential firing threshold) and all the connection properties at the *first order*.[14] More precisely: P_{n1} is the type of the neuron n, so $P_{n1} = 1$ if the neuron n is an excitatory neuron and -1 otherwise. $P_{n2} = \frac{V_n^* - \langle V^* \rangle}{\Delta V^*}$ if $\Delta V^* > 0$ and 0 otherwise. P_{n3} is number of excitatory neurons connected to the axon of neuron n (this means the number of excitatory sons of the neuron n, see Section 2.1) and P_{n4} the number of inhibitory sons. Identically, P_{n5} is the number of excitatory fathers of the neuron n and P_{n6} the number of inhibitory fathers.

Our linear least squares method, like in Wilkinson and Reinsch (1971), consists in finding a vector $\vec{x} = \{x_i\}_{i=1,\dots,6}$ such that the euclidean norm

$$\left\| P\vec{x} - \vec{\alpha} \right\| \tag{5}$$

is minimized. This particular $\vec{x}$ gives us the relations (at the linear order) between the six first order properties[15] of a neuron (in our simulations) and its leadership score.

By repeating the calculation (Eq. (5)) for each simulation and averaging over all simulations, we obtain the typical solution

$$\vec{x} = (1.2 \pm 0.3,\ -2.3 \pm 0.4,\ 0.13 \pm 0.03,\ -0.19 \pm 0.04,\ -0.13 \pm 0.03,\ 0 \pm 0.03)^T . \tag{6}$$

Equation (6) means that a good prediction p_n for the leadership score α_n of the neuron n in a network is given by

$$p_n = 1.22 \cdot P_{n1} - 2.33 \cdot P_{n2} + 0.13 \cdot P_{n3} - 0.19 \cdot P_{n4} - 0.13 \cdot P_{n5}, \tag{7a}$$

$$\text{if } \Delta V^* > 0: \quad p_n = 1.22 \cdot \text{excitatory}_n - 2.33 \cdot \frac{V_n^* - \langle V^* \rangle}{\Delta V^*} + 0.13 \cdot \#\,\text{excitatory sons}_n - 0.19 \cdot \#\,\text{inhibitory sons}_n - 0.13 \cdot \#\,\text{excitatory fathers}_n \tag{7b}$$

where $(\text{excitatory}_n =)\ P_{n1} = 1$ if the neuron n is an excitatory neuron and -1 otherwise, $P_{n2} = \frac{V_n^* - \langle V^* \rangle}{\Delta V^*}$ if $\Delta V^* > 0$ and 0 otherwise, $P_{n3}\ (= \#\,\text{excitatory sons}_n)$ is the number of excitatory sons (of neuron n), $P_{n4}\ (= \#\,\text{inhibitory sons}_n)$ is the number of inhibitory sons and $P_{n5}\ (= \#\,\text{excitatory fathers}_n)$ is the number of excitatory fathers.

In Eq. (5), the $\vec{x}$ is unique if and only if the rank of $P^T P$ is six (the number of components of $\vec{x}$) (Golub and Van Loan 1996). But, in some simulations, it is possible that, for example, $\Delta V^* = 0$ then the rank of $P^T P$ is lower than six. However, we must precise that, in the particular case $\Delta V^* = 0$, the prediction p_n does not depend on V_n^* (trivial since $P_{n2} = 0$ for all n). So, the problem should be restricted by removing the second column of P and by computing only five components of $\vec{x}$. The final prediction p_n (Eq. (7)) remains the same since "the missing component" has no physical meaning and will be multiplied by 0 in the prediction p_n (Eq. (7)). Each component of Eq. (6) is computed by averaging over all simulations in which the considered component has a physical meaning. All the components of Eq. (6) have a relative error of about 20%.

Note also that Eq. (7) do not depend on the axon length distribution. Furthermore, by building a random

[14] We call connection properties at the first order all the direct connections of the neuron in the network contained in the matrix of synaptic weights W (this means the number of sons and fathers (see Section 2.1)). In particular, we do not introduce any information about higher order properties, such as the number of paths between two neurons. All these higher order properties are obtained from W above.

[15] We call first order properties all the neuron properties and all the connection properties at the first order.

network with a uniform probability of connections (see footnote 10) (i.e., fixing only the mean number of connections per neuron) we obtain the same formula.

Precisely, Eq. (7) mean that a typical leader in our simulations is an excitatory neuron, that it has a low membrane potential firing threshold and that it has a lot of excitatory sons but a few inhibitory sons and a few excitatory fathers. Equation (7) in this exact form is valid for a mean number of connections per neuron of about eleven ($\langle$# connections/neuron$\rangle \cong 11$). Equation (7) was computed for networks in which $N \gg \langle$# connections/neuron$\rangle$ and are typically valid in these cases. In particular Eq. (7) shows that the prediction p_n does not depend on the number of neurons N.

By looking at Fig. 4(a), one can think that the only property among the five that is really necessary for a neuron to be a leader is the low membrane potential firing threshold. However, this property cannot be the only one since:

1. An inhibitory neuron cannot be a leader because it cannot create a burst (Fig. 5(a)).
2. A neuron without output cannot create a burst (trivial).
3. A neuron with many inputs is necessarily more often a follower than a trigger (Fig. 5(b)).

So, even if it is obvious that a neuron needs more than one property to be a leader and that Eq. (7) give explicitly the five needed properties with their relative importance, we can have a look at Figs. 5 and 8. These figures complete the picture given by Fig. 4(a), in a way to illustrate Eq. (7).

A comparison of the correlation coefficient of the linear regression presented in Figs. 8(a) and 9 illustrates that, in a network in which all the neurons have the same membrane potential firing threshold (i.e., $\Delta V^* = 0$), the importance of the number of excitatory sons (P_{n3}) in the leadership score becomes significantly stronger. This means that the relative importance of the number of excitatory sons (P_{n3}) in the prediction p_n (Eq. (7)) is somewhat hidden by the first importance of the low membrane potential firing threshold. The relative importance of the different coefficients in the prediction p_n (Eq. (7)) is clearly highlighted by the absolute value of these coefficients and illustrated by the Figs. 4, 5, 8 and 9. Moreover, the relative importance of each term of Eq. (7) varies with the parameters.

It is important to remark that in Figs. 8(a) and 9 some of the best leaders are concentrated near the mean number of excitatory sons, unlike what is first expected by our prediction p_n (Eq. (7)). However, Figs. 8(a) and 9 represent a projection of a multidimensional figure that we cannot present in this paper for obvious reasons. This multidimensional figure would represent very well our prediction formula (Eq. (7)) by representing the leadership score α as a function

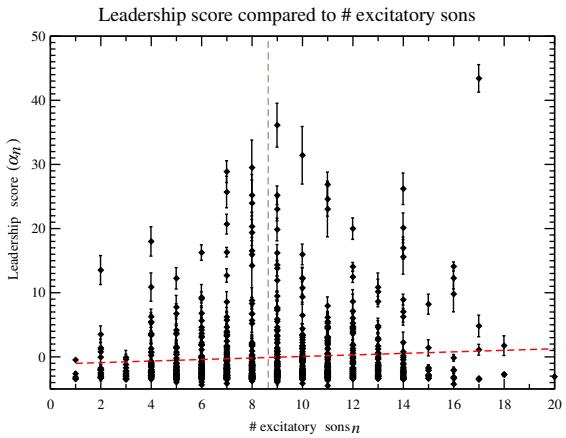

(a) The leadership score (α_n) compared to the number of excitatory sons. The *red dashed line* is a linear regression with correlation $r^2 \cong 0.09$ that shows that, on average, a higher number of excitatory sons implies an higher leadership score. The mean number of excitatory sons per neuron is represented by the *brown dashed line*.

(b) The leadership score (α_n) compared to the number of inhibitory sons. The *red dashed line* is a linear regression with correlation $r^2 \cong -0.14$ that shows that, on average, a higher number of inhibitory sons implies an lower leadership score. The mean number of inhibitory sons per neuron is represented by the *brown dashed line*.

Fig. 8 Illustration of the importance of the number of sons in the leadership score. As usual, the error bars of each point in this figure are computed using five simulations done with the same network and parameters. The parameters are the same than in Fig. 4: $N = 900$, $\mathsf{r} = 0.85$, $L = 7$, $r = 0.2$, $\Delta V^* = 0.1$, $v = 5\frac{1}{\text{ms}}$, $\mathsf{w} = 0.1$, $\tau = 100$ ms, $\sigma = 0.008$, $\omega = 0.001$ s, $n_{\text{burst}} = 100$, $\delta t_{\text{burst}} = 15$ ms and $\delta t_{\text{isolate}} = 5$ ms

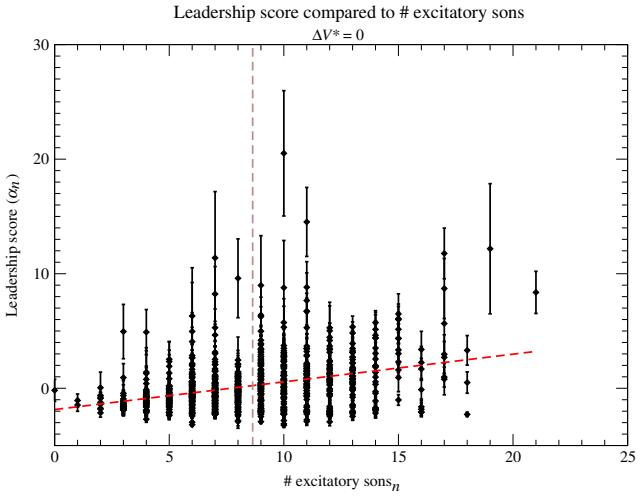

Fig. 9 As Fig. 8(a) compares the leadership score (α_n) to the number of excitatory sons, but here $\Delta V^* = 0$. The *red dashed line* which is a linear regression has therefore a better correlation $r^2 \cong 0.35$. The mean number of excitatory sons per neuron is represented by the *brown dashed line*. As usual, the error bars of each point in this figure are computed using five simulations done with the same network and parameters. Parameters: $N = 900$, $\mathsf{r} = 0.85$, $L = 7, r = 0.2$, $\Delta V^* = 0$, $\upsilon = 5\ \frac{1}{\text{ms}}$, $\tau = 100$ ms, $\mathsf{w} = 0.1$, $\sigma = 0.008$, $\omega = 0.001$ s, $n_{\text{burst}} = 100$, $\delta t_{\text{burst}} = 15$ ms and $\delta t_{\text{isolate}} = 5$ ms

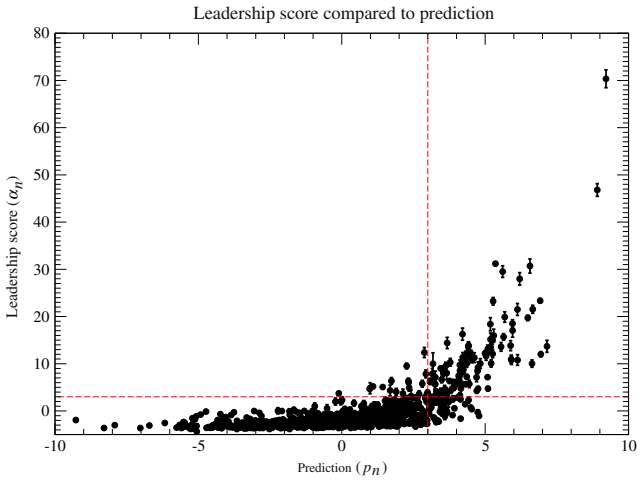

Fig. 10 The leadership score (α_n) compared to the prediction (p_n) for a particular simulation. The *red dashed lines* separate leaders and non-leaders for both the simulation and the prediction. As usual, the error bars of each point in this figure are computed using five simulations done with the same network and parameters. Parameters: $N = 900$, $\mathsf{r} = 0.85$, $L = 7, r = 0.2$, $\Delta V^* = 0.1$, $\upsilon = 5\ \frac{1}{\text{ms}}$, $\tau = 100$ ms, $\mathsf{w} = 0.1$, $\sigma = 0.0081$, $\omega = 0.001$ s, $n_{\text{burst}} = 100$, $\delta t_{\text{burst}} = 15$ ms and $\delta t_{\text{isolate}} = 5$ ms

of all the considered parameters (number of excitatory sons/fathers, membrane potential firing threshold V^*, ...). Since in a projection like Fig. 9 (or Fig. 8(a)) only the number of excitatory sons parameter is represented, then the other parameters are, in mean, projected near the mean number of excitatory sons.

Now, considering a given neural network (that we did not use to obtain Eq. (7)) and using Eq. (7), we can predict, even before running our simulation, which neurons will be leaders. Figure 10 shows a typical prediction. Remark that this prediction is pretty reliable because: All the neurons with a prediction p_n lower than 0 are indeed not leaders and all the neurons with a prediction p_n bigger than 6 are leaders ($\alpha_n > 3$). More precisely, in Fig. 10, the prediction efficiency[16] p_e is 0.93. This means that the prediction is correct for more than 90% of the neurons ($p_e > 0.9$).

Regarding the figures, one can understand that the prediction p_n (Eq. (7)) expresses a tendency but not a strict rule. Moreover, one can probably find examples of networks in which most of the neurons have a prediction (Eq. (7)) higher than 3. However, these examples are mostly out of the parameter range defined in Section 2.2 in which the prediction p_n is typically valid.

For further analysis, Table 3 shows the prediction efficiency (see footnote 16) for different simulations. Most of the simulations presented in Table 3 show that the trend of prediction of Eq. (7) is correct ($p_e > 0.9$). Precisely, for a range of simulations with different standard deviations of the membrane potential firing threshold (ΔV^*) (Table 3 simulations B, D, E and F), for different mean noises (σ) and exponential clock rates (ω) (Table 3 simulations C and F) the trend of prediction is correct. So, by looking only at the simulations B, C, D, E, F, G and H of Table 3, we can say that Eq. (7) give a pretty good prediction (even without adapting the coefficient of Eq. (7) with the dynamical parameters).

Before discussing the prediction efficiency of the simulation A, let us comment the good results obtained with the simulations G and H. The network of the simulation G is a random network with a uniform probability of connections (see footnote 10) while the network of the simulation H is an homogeneous network.[17] Both simulations (G and H) are not built as described in

[16] We call prediction efficiency the coefficient $p_e = \frac{\sum_n \text{correct prediction}_n}{N}$ where correct prediction$_n$ is 1 if the neuron n is a leader $\alpha_n > 3$ (respectively not a leader $\alpha_n \leq 3$) in the simulation and its prediction $p_n > 3$ (respectively $p_n \leq 3$), otherwise: correct prediction$_n = 0$.

[17] This means a network in which all neurons have exactly the same number of connections: the eight nearest neighbors (unlike Fig. 1). However, the membrane potential firing threshold of the neurons differs.

Table 3 The prediction efficiency p_e for different simulations

Simulation	Type	r	w	ΔV^*	σ	ω (s)	p_e
A	r, L	0	0.0666	0.1	0.008	0.001	0.88
B	r, L	0.2	0.1	0.05	0.008	0.001	0.92
C	r, L	0.2	0.1	0.1	0.014	0.002	0.92
D	r, L	0.2	0.1	0	0.008	0.001	0.91
E	r, L	0.2	0.1	0.2	0.007	0.001	0.91
F	r, L	0.2	0.1	0.1	0.008	0.001	0.93
G	Random	0.2	0.1	0.1	0.008	0.001	0.93
H	Homogeneous	0.2	0.12	0.05	0.008	0.001	0.93

$p_e = \frac{\sum_n \text{correct prediction}_n}{N}$ where correct prediction$_n$ is 1 if the neuron n is a leader $\alpha_n > 3$ (respectively not a leader $\alpha_n \leq 3$) in the simulation and its prediction $p_n > 3$ (respectively $p_n \leq 3$), otherwise: correct prediction$_n = 0$. Parameters: r $= 0.85$, $L = 7$, common: $N = 900$, $v = 5\ \frac{1}{\text{ms}}$, $\tau = 100$ ms, $n_{\text{burst}} = 100$, $\delta t_{\text{burst}} = 15$ ms and $\delta t_{\text{isolate}} = 5$ ms

Section 2.1, nevertheless both simulations have stable leaders[18] and have a correct trend of prediction given by Eq. (7). An additional comment on the case of the simulation H might be useful. By an homogeneous network, we do not mean a network in which all the neurons are the same,[19] since obviously, in such a case, we would not observe stable leaders. But the probability of such a symmetry (see footnote 19) appearing in our model is zero. Nevertheless, it is possible to construct examples in which the prediction (Eq. (7)) is almost identical for every neuron and can be bigger than 3. This is not a paradox since these examples are not built in accordance with Section 2.2.

For the simulation A the trend of prediction is less good ($p_e \leq 0.9$). The fact is the following, for the simulation A, the inhibitory proportion r equals 0. This means that for simulation A we did not stay in the parameters range that we gave in Section 2.2 and that we used to find out Eq. (7). We can say that the fact that Eq. (7) does not give a very good trend of predictions for the simulation A is a kind of edge effect.[20] With $\vec{x}_{r=0} = (-0.8927, -3.23, 0.07, \lambda_1, -0.02, \lambda_2)^T$ in Eq. (7) (where $\lambda_1, \lambda_2 \in \mathbb{R}$), we obtain a much better prediction for simulation A ($p_e = 0.92$). Remark that the first number (-0.8927) (the coefficient of $P_{n1} =$ excitatory$_n$) of $\vec{x}_{r=0}$ has no physical meaning because all neurons are excitatory neurons (if $r = 0$ then $P_{n1} =$ excitatory$_n = 1\ \forall n$). For the same reason λ_1, λ_2 in $\vec{x}_{r=0}$ can be any real number because P_{n4} (=# inhibitory son$_n$) and P_{n6} (=# inhibitory fathers$_n$) are always 0 if all neurons are excitatory neurons.

All this means that the relative importance of the leader properties change by changing the parameters of the simulation but the trend in Eq. (7) is correct (this fact was already discussed while comparing Figs. 8(a) and 9). By a correct trend we mean that $P_{n2} = \frac{V_n^* - \langle V^* \rangle}{\Delta V^*}$ (if $\Delta V^* > 0$ and 0 otherwise) and P_{n3} (=# excitatory sons$_n$) are still in the range of the value given by Eq. (6) if we consider three times (or less) the standard deviation.[21] The only significant deviation to the mean is observed for P_{n5} (=# excitatory fathers$_n$). This means that when $r = 0$ the number of excitatory fathers is less relevant for the leadership than in the standard case $r = 0.2$. However, we observed that the sign of each coefficient in Eq. (7) is robust (as soon as the coefficient has a physical meaning). This means that only the coefficients of the prediction formula can change while we vary the parameters.

To illustrate once again the relative importance of each term of Eq. (7) we continue with Table 3; we can easily understand that P_{n2} (for example) is very important for the simulation E ($\Delta V^* = 0.2$) while P_{n2} is irrelevant for the simulation D ($\Delta V^* = 0$).

We next explain why we do not use a bigger matrix P. Considering a given neural network, we can extract many different properties for all neurons n: the number of fathers, the number of sons, the number of fathers'fathers (second order property[22]), the number of loops (order $2, 3, 4, 5 \ldots$) in which the neuron n participates,... We can also reduce the network to an excitatory network and so on. We can as well try to

[18] This fact was already explained in Section 4.2.

[19] All the neurons with the same membrane potential firing threshold, type and number of fathers and sons.

[20] Our model was done to mimic *in vitro* experiments (Eckmann et al. 2008) in which the inhibitory proportion r is about 20%. Normally $0 \leq r \leq 1$. So by choosing $r = 0$ we are in the edge of the parameter space. That is why we pretend that the abnormally high prediction error is a kind of edge effect.

[21] In a Gaussian distribution, which is expected for the components of $\vec{x}$, the interval that contains the mean value more or less three times the standard deviation includes 99% of the results.

[22] This means that we need to compute W^2 to extract this property.

improve our results by using a lot of tricks and/or cutoff. But using the properties at the first order (see footnote 14) seems to be an easy and logical way of doing. This is true especially considering two facts: (1) A son will not necessarily fire after one of his fathers did, so what to say about the sons of this son? (2) The leadership score depends on the dynamical parameters. Taking that fact into account improves the results more than considering the second order properties in the network.

To conclude, Eq. (7) cannot be taken as a general law and Eq. (7) is only a good approximation of the leadership score in the range of parameters we chose in Section 2.2. However, we have observed that the signs in Eq. (7) are robust under the change of parameters. This means that our typical leader profile is the right one.

Even if Eq. (7) is computed on small scale simulations, the trend of the typical leader profile is the correct one. Even more, we propose to use the following leader profile if the mean number of connections per neuron varies

if $r, \Delta V^* > 0$:

$$p_n = 1.22 \cdot \text{excitatory}_n - 2.33 \cdot \frac{V_n^* - \langle V^* \rangle}{\Delta V^*} + 1.14 \cdot \frac{\#\text{ excitatory sons}_n}{(1-r)\langle \#\text{ connections/neuron} \rangle} - 0.42 \cdot \frac{\#\text{ inhibitory sons}_n}{r\,\langle \#\text{ connections/neuron} \rangle} - 1.14 \cdot \frac{\#\text{ excitatory fathers}_n}{(1-r)\langle \#\text{ connections/neuron} \rangle}. \quad (8)$$

This equation was computed knowing that in Eq. (7): $\langle \#\text{ connections/neuron} \rangle = 11$.

We have already explained in Section 4.2 that we can observe leaders in our simulations as soon as we use "reasonable" (see footnote 9) parameters. Further more, considering a given simulation, we can store the neurons using the leadership score. After that, if we decide to remove some of the (best) leaders from the network and then run again our simulation we still observe stable leaders. Finally, in a leaky integrate and fire neuron model there are leaders in the networks and the neurons which fit better with the typical leader profile are the leaders.

4.4 First to fire neurons

In this section we characterize the first to fire neurons. From this point, we will call first to fire neurons the neurons that fire in a short time after the trigger. This means that the first to fire neurons fire roughly in the successful pre-burst.

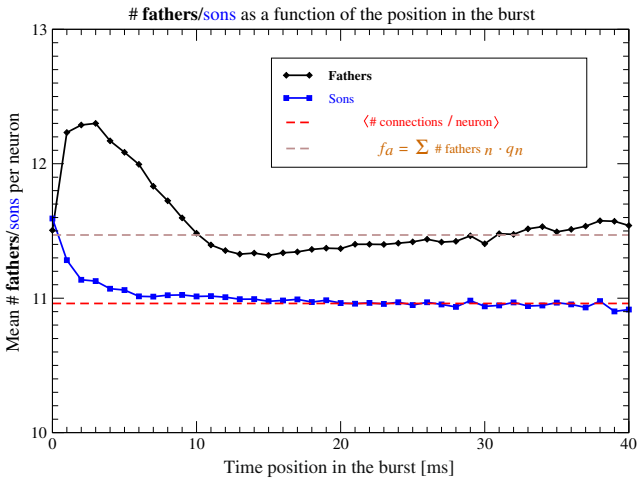

Fig. 11 The mean number of fathers/sons per neuron as a function of the time position of a spike of this neuron in the burst. The time bin in which we average the number of fathers/sons per neuron is 1 ms. The time position 0 is reserved for the trigger of the burst. The mean number of connections per neuron in the network (noted $\langle \#\text{ connections/neuron} \rangle$) is about 11. The typical number of fathers of an active neuron f_a is about 11.5 (see Eq. (9) for definition). We obtained this figure by averaging over more than 35,000 bursts. Parameters: $N = 900$, $\mathsf{r} = 0.85$, $L = 7$, $r = 0.2$, $\Delta V^* = 0.05$, $\upsilon = 5\ \frac{1}{\text{ms}}$, $\mathsf{w} = 0.1$, $\tau = 100$ ms, $\sigma = 0.008$, $\omega = 0.001$ s, $n_{\text{burst}} = 150$, $\delta t_{\text{burst}} = 15$ ms and $\delta t_{\text{isolate}} = 5$ ms

Figure 11 shows the mean number of fathers (or sons) per neuron as a function of the time position of a spike of this neuron in the burst. To obtain Fig. 11 we average over all the bursts of a given simulation without taking into account if the trigger of the burst was a leader or not. Nevertheless, when we look at the mean number of sons per trigger[23] we remark that the trigger of the burst has, on average, more sons than its followers. This fact is consistent with our previous analysis. Remember that Fig. 4(b) shows that leaders trigger more bursts than other neurons. This means that the trigger is, on average, a leader. Remember also that Eq. (7) tells that a leader has typically many excitatory sons (this means a lot of sons as well).

Figure 11 also shows that the first to fire neurons have, on average, more sons than their followers and have, on average, less sons than the trigger. This means that very often several leaders are present in the successful pre-burst (this is linked with the triggering force of leaders, data not shown, see Zbinden 2010). So the

[23]The time position 0 in Fig. 11 is reserved for the trigger of the burst.

fact that first to fire neurons have typically a lot of sons is consistent with Eq. (7).

In Fig. 11 the mean number of sons per neuron tends to the mean number of connections per neuron in the network. This means that, except for the trigger and the first to fire neurons, the mean number of sons per neuron for the neurons which fire during the burst itself is not relevant.

Figure 11 shows explicitly that the mean number of fathers per neuron of the first to fire neurons is higher than the mean number of connections per neuron in the network. This means that the first to fire neurons are characterized by a high number of fathers. This is consistent with the fact that neurons with a lot of fathers light up early in the burst, respectively in the successful pre-burst (see Cohen et al. 2009). In facts neurons with a lot fathers have an higher neural activity than neurons with a few fathers (data not shown). And again, this is consistent with Cohen et al. (2009) and Fig. 11 which shows that active neurons in the burst are, on average, neurons with a lot of fathers (typically more fathers than the mean number of connections per neuron in the network).

In Fig. 11 the mean number of fathers per neuron (unlike the mean number of sons) does not tend to the mean number of connections per neuron in the network but seems to increase again after the decay of the first to fire neurons. This is consistent with the following fact: in a burst, after a while, neurons are able to fire again (as soon as their membrane potentials are charged enough). And, of course, the neurons with a lot of fathers are able to fire again sooner than the others.

What about the mean number of fathers of the trigger? Figure 11 shows a tendency of the trigger to have more fathers than the mean number of connections per neurons. This last fact seems to contradict our predictions (Eq. (7)). But in Fig. 11 the mean number of fathers of the trigger is approximately what we call the typical number of fathers of an active neuron f_a:

$$f_a = \sum_{n=1}^{N} \#\,\text{fathers}_n \cdot q_n \tag{9}$$

where $\#\,\text{fathers}_n$ is the number of fathers of neuron n and q_n is the neural activity ratio of neuron n. Figure 11 shows that (except for the first to fire) the mean number of fathers per neuron is about f_a the typical number of fathers of an active neuron and shows that the number of fathers of the typical trigger is not different from f_a. These two facts can explain the term concerning the number of fathers in Eq. (7), but still we can think it contradicts Eq. (7).

To clarify this conflict, let us have a look at Fig. 12. This figure shows, as Fig. 11, the mean number of fathers (and sons) per neuron as a function of the time position of a spike of this neuron in the burst. In Fig. 12 the standard deviation of the membrane potential firing threshold ΔV^* is much higher than the one in Fig. 11. In Fig. 12, we see that the number of sons of the trigger as well as the one of the first to fire neurons is higher than the mean number of connections per neuron in the network. And we see that the number of fathers of the trigger is lower than the mean number of connections per neuron in the network. But the number of fathers of the first to fire neurons is higher than the mean number of connections per neuron in the network. This forces us to conclude that the simulation shown in Fig. 12 does not contradict Eq. (7). The reason for that is that the membrane potential firing threshold plays a more important rôle in this case.

We can also remark that in Fig. 11 like in Fig. 12, the mean number of fathers per neuron tends approximately to the typical number of fathers of an active neuron f_a while we look forward in time in the burst.

Now, let us clarify the observation of Fig. 3 concerning the neurons 634 and 643. Neuron 643 is one of the best leaders of the simulation of Fig. 3(b) while restricting the observation to 60 neurons only implies

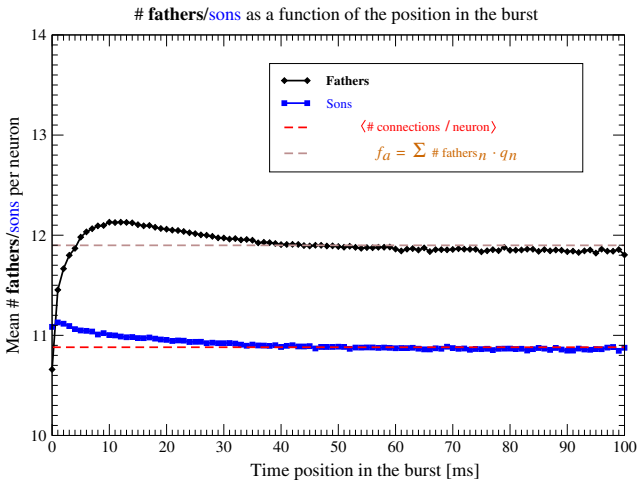

Fig. 12 The mean number of fathers/sons per neuron as a function of the time position of a spike of this neuron in the burst. The time bin in which we average the number of fathers/sons per neuron is 1 ms. The time position 0 is reserved for the trigger of the burst. The mean number of connections per neuron in the network (noted ⟨# connections/neuron⟩) is about 11. The typical number of fathers of an active neuron f_a is about 11.9 (see Eq. (9)) for definition). We obtained this figure by averaging over more than 35,000 bursts. Parameters: $N = 900$, $\mathsf{r} = 0.85$, $L = 7$, $r = 0.2$, $\Delta V^* = 0.2$, $\upsilon = 5\ \frac{1}{\text{ms}}$, $\mathsf{w} = 0.1$, $\tau = 100$ ms, $\sigma = 0.007$, $\omega = 0.001$ s, $n_{\text{burst}} = 150$, $\delta t_{\text{burst}} = 15$ ms and $\delta t_{\text{isolate}} = 5$ ms

that neuron 634, which is not a leader (see Fig. 3(b)), appears as a leader (see Fig. 3(a)). The fact is that both neurons 634 and 643 have the profile of first to fire neurons (mean number of fathers close to the typical number of fathers of an active neuron). But the membrane potential firing threshold of the two neurons explains why only neuron 643 can be a leader: $V^*_{634} = 1.009$ and $V^*_{643} = 0.869$ ($\langle V^* \rangle = 1$ and $\Delta V^* = 0.05$). So while restricting the observation to 60 neurons only, it is possible that the first to fire neurons appear as leaders. In the experiments (Eckmann et al. 2008) it was impossible to distinguish between true leaders and first to fire neurons.

Finally we have a competition between two facts: To be a leader, a neuron needs to be able to fire early (in order to do that it must have a low membrane potential firing threshold and a lot of fathers) and to be a leader, a trigger must trigger more bursts than we expect. Typically a leader has a good triggering power (this means a lot of excitatory sons) and a relatively low neural activity ratio (this means less fathers than the typical number of fathers of an active neuron). That is the message of Eq. (7) (respectively Eq. (8)). Remember that Eq. (7) was obtained by averaging over simulations, so Eq. (7) express only a tendency of what kind of neurons the leaders are.

5 Conclusion

Experimental studies show the existence of leader neurons in population bursts of 2D living neural networks (Eytan and Marom 2006; Eckmann et al. 2008). This leads naturally to a question: Do leaders also exist in neural network models? In this study, we have proved that stable leaders exist in leaky integrate and fire neural network simulations (lIF).

More precisely, we have clearly shown that a single specific neuron (the leader) can start an electrical activity (successful pre-burst) and that the followers (the first to fire neurons) transmit this activity to the (almost) full network. So the leaders do not really act alone but only initiate the successful pre-burst.

In our simulations, we saw that leaders depend on the network but also on the dynamical parameters. Because the leaders mainly depend on the network and on the own properties of the neurons, we were able to find some important properties for these leaders. Firstly, they are excitatory neurons and have a low membrane potential firing threshold (ability of firing early). Secondly, they send a signal to a lot of excitatory neurons and to a few inhibitory neurons (triggering power). Finally, they receive only a few signals from other excitatory neurons (leaders trigger more bursts than we expect by looking at the neural activity).

To conclude, we studied neural networks which are complex systems. We have shown that in lIF some neurons are leaders because of their position in the network (many outputs for example). The fact that the most important properties to become a leader are only what we call first order (see footnote 14) properties is a strong result. This means that the second order connections do not play a significant rôle, as if for these connections (and those of higher rank) a mean field approximation suffices.

Others simple models can highlight the leader properties (Eckmann et al. 2010). Moreover, the study of more biological plausible models (Izhikevich 2004; Gerstner and Naud 2009) (like Hodgkin–Huxley) would be very interesting to explore too and could probably also produce stable leaders. These models could probably be used to find out other leader properties.

Acknowledgements I would like to thank Jean-Pierre Eckmann, my PhD advisor at the University of Geneva, Switzerland, for his continuous useful help along this study. This paper could not have been without the help of Elisha Moses, Weizmann Institute of Science, Israel. During all this research, I was supported by the Fonds National Suisse. Finally I would like to thank Sonia Iva Zbinden.

References

Alvarez-Lacalle, E., & Moses, E. (2007). Slow and fast pulses in 1-D cultures of excitatory neurons. *Journal of Computational Neuroscience, 26*(3), 475–493.

Brette, R., & Gerstner, W. (2005). Adaptive exponential integrate-and-fire model as an effective description of neuronal activity. *Journal of Neurophysiology, 94*, 3637–3642.

Cessac, B. (2008). A discrete time neural network model with spiking neurons. Rigorous results on the spontaneous dynamics. *Journal of Mathematical Biology, 56*(3), 311–345.

Cessac, B., Rochel, O., & Viéville, T. (2008). *Introducing numerical bounds to event-based neural network simulation*. arXiv:0810.3992.

Cessac, B., & Samuelides, M. (2007). From neuron to neural network dynamics. *EPJ Special Topics, 142*(1), 7–88.

Cohen, O., Keselman, A., Moses, E., Rodriguez Martinez, M., Soriano, J., & Tlusty, T. (2009). Quorum percolation in living neural networks. *A Letters Journal Exploring the Frontiers of Physics, 89*. doi:10.1209/0295-5075/89/18008.

Droge, M. H., Gross, G. W., Hightower, M. H., & Czisny, L. E. (1986). Multielectrode analysis of coordinated, multisite, rhythmic bursting in cultured CNS monolayer networks. *Journal of Neuroscience, 6*(6), 1583–1592.

Eckmann, J.-P., Feinerman, O., Gruendlinger, L., Moses, E., Soriano, J., & Tlusty, T. (2007). The physics of living neural networks. *Physics Reports, 449*, 54–76.

Eckmann, J.-P., Jacobi, S., Marom, S., Moses, E., & Zbinden, C. (2008). Leader neurons in population bursts of 2D living neural networks. *New Journal of Physics, 10*(015011).

Eckmann, J.-P., Moses, E., Stetter, O., Tlusty, T., & Zbinden, C. (2010). Leaders of neuronal cultures in a quorum percolation model. *Frontiers in Computational Neuroscience, 4*(132).

Eckmann, J.-P., & Tlusty, T. (2009). Remarks on bootstrap percolation in metric networks. *Journal of Physics A: Mathematical and Theoretical, 42*(205004).

Eytan, D., & Marom, S. (2006). Dynamics and effective topology underlying synchronization in networks of cortical neurons. *Journal of Neuroscience, 26*(33), 8465–8476.

Gerstner, W., & Kistler, W. M. (2002). *Spiking neuron models. Single neurons, populations, plasticity*. Cambridge: Cambridge University Press.

Gerstner, W., & Naud, R. (2009). How good are neuron models? *Science, 326*, 379–380.

Golub, G. H., & Van Loan, C. F. (1996). *Matrix computations* (3rd ed.). Baltimore: The Johns Hopkins University Press.

Izhikevich, E. M. (2004). Which model to use for cortical spinking neurons? *IEEE Transactions on Neural Networks, 15*(5), 1063–1070.

Luscher, H.-R., Jolivet, R., Rauch, A., & Gerstner, W. (2006). Predicting spike timing of neocortical pyramidal neurons by simple threshold models. *Journal of Computational Neuroscience, 21*, 35–49.

Maeda, E., Robinson, H. P., & Kawana, A. (1995). The mechanisms of generation and propagation of synchronized bursting in developing networks of cortical neurons. *Journal of Neuroscience, 15*(10), 6834–6845.

Naud, R., Marcille, N., Clopath, C., & Gerstner, W. (2008). Firing patterns in the adaptive exponential integrate-and-fire model. *Biological Cybernetics, 99*, 335–347.

Rudolph, M., & Destexhe, A. (2007). How much can we trust neural simulation strategies? *Neurocomputing*, (70), 1966–1969.

Soriano, J., Rodriguez Martinez, M., Tlusty, T., & Moses, E. (2008). Development of input connections in neural cultures. *Proceedings of the National Academy of Sciences of the United States of America, 105*(37), 13758–13763.

Tscherter, A., Heuschkel, M. O., Renaud, P., & Streit, J. (2001). Spatiotemporal characterization of rhythmic activity in rat spinal cord slice cultures. *European Journal of Neuroscience, 14*(2), 179–190.

Wagenaar, D. A., Pine, J., & Potter, S. M. (2006a). An extremely rich repertoire of bursting patterns during the development of cortical cultures. *BMC Neuroscience, 7*(11).

Wagenaar, D. A., Pine, J., & Potter, S. M. (2006b). Searching for plasticity in dissociated cortical cultures on multi-electrode arrays. *Journal of Negative Results in Biomedicine, 5*(1), 16.

Wilkinson, J. H., & Reinsch, C. (1971). *Linear algebra*. Berlin: Springer.

Zbinden, C. (2010). *Leader neurons in living neural networks and in leaky integrate and fire neuron models*. PhD thesis, University of Geneva. http://archive-ouverte.unige.ch/unige:5451.